

Electrochemically Programmed Release of Biomolecules and Nanoparticles

Prashant Mali,[†] Nirveek Bhattacharjee,[†] and Peter C. Searson^{*‡}

The Whitaker Biomedical Engineering Institute and the Department of Materials Science and Engineering, Johns Hopkins University, Baltimore, Maryland 21218

Received April 25, 2006

ABSTRACT

The controlled release of molecules or nanoparticle conjugates is an important tool for a wide range of applications in science and engineering. Here we demonstrate electrochemically programmed release of biomolecules and nanoparticles immobilized on patterned gold electrodes using the thiol–gold linkage. This technique exploits the reductive desorption of self-assembled monolayers and allows both spatially controlled release and regeneration of small molecules (e.g., drugs), biopolymers (e.g., peptides, proteins, DNA), protein assemblies (e.g., viruses), and nanoparticles (e.g., particle–DNA conjugates). Fluorescence microscopy is used to image the release of avidin and nanoparticles in phosphate-buffered saline and to determine the kinetics of desorption. We also demonstrate that the electrodes can be regenerated using the same conjugation scheme.

Many applications in science and engineering require the controlled release of small quantities of molecules or nanoparticle conjugates. Current approaches include microfluidic arrays, encapsulated polymers, and microfabricated reservoirs with dissolvable lids. Electrochemical desorption of self-assembled monolayers offers a powerful tool for the programmed release of immobilized molecules (e.g., drugs, peptides, proteins, DNA, and viruses) and nanoparticles from an electrode surface. Since the molecules or particles are anchored to a surface in a monolayer, patterning techniques can be used to provide spatial control of the release of one or more molecules or particles and of very small quantities. Furthermore, the electrodes can be regenerated and hence can be used for multiple release cycles. We expect this technique to find application in fields such as controlled drug release devices,¹ gene expression platforms,² programmable DNA/protein arrays,³ protein purification systems,⁴ and microreactors.⁵ Here we demonstrate the controlled release and regeneration of proteins and nanoparticles tethered to gold electrode arrays through a thiol linkage.

A schematic illustration of electrochemically programmed release is shown in Figure 1. The molecule or nanoparticle of interest is tethered to the gold electrode using a thiol linkage. In the first step, a self-assembled monolayer (SAM) of a thiol terminated with a coupling group (e.g., amine) is formed on a gold electrode. A suitable receptor with a variable length spacer can then be attached via the coupling group (e.g., using a terminal succinimide group). Finally,

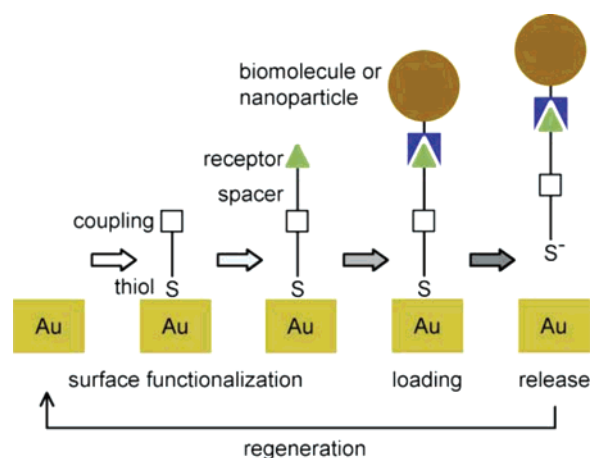
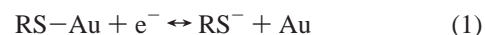


Figure 1. Schematic illustration of surface functionalization, loading of molecules or nanoparticles, electrochemically programmed release, and electrode regeneration.

the molecule or nanoparticle is attached to the receptor. The thiol bond is strong ($\approx 168 \text{ kJ mol}^{-1}$),⁶ but is electrochemically reversible, i.e., thiols can be electrochemically desorbed from the gold surface to form the thiolate



The potential at which desorption occurs is dependent on the chain length and the nature of the tail group, as well as on pH.^{7–9} Thus, applying a potential negative to the desorption potential releases the bound SAM. The spacer can also be modified to include a cleavable (e.g., disulfide)

* Corresponding author. E-mail: searson@jhu.edu.

[†] The Whitaker Biomedical Engineering Institute; both authors contributed equally.

[‡] Department of Materials Science and Engineering.

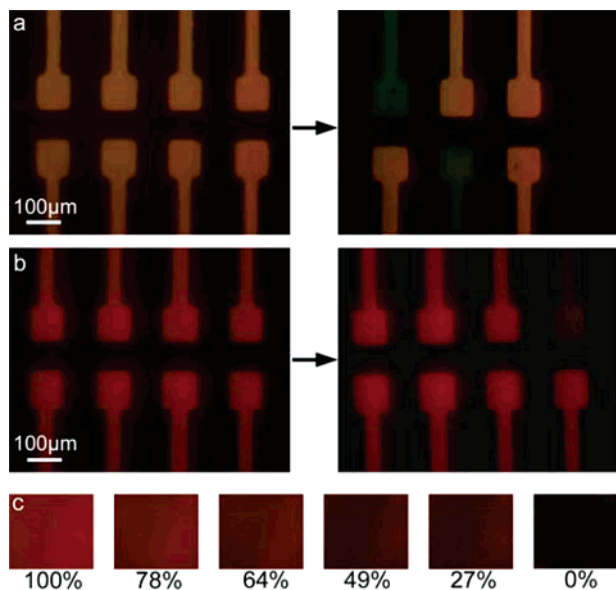


Figure 2. Fluorescence images showing electrochemically programmed release of (a) proteins (avidin) and (b) nanoparticles (40 nm diameter, avidin conjugated polystyrene nanoparticles), from selected micropatterned gold electrodes. (c) Fluorescence images of an avidin functionalized electrode showing the fluorescence as a function of coverage during desorption.

or biodegradable (e.g., ester) group to facilitate the further dissociation of the molecule or particle from the desorbed complex.

In Figure 2 we apply this concept to the electrochemically programmed release of proteins and nanoparticles. Figure 2a shows fluorescence images of an electrode array before and after electrochemically programmed release of avidin. Rhodamine-conjugated avidin was attached to lithographically patterned gold electrodes through a biotin-terminated thiol. First, a monolayer of amine-terminated thiol (11-amino-1-undecane-thiol) was formed on the gold electrodes. A succinimide-terminated biotin linker (succinimidyl-6-(biotinamido)-6-hexanamidohexanoate) was then reacted with the terminal amine groups of the thiol SAM. The conjugation reaction was carried out at pH 7.4–8.4 so that the fraction of reactive (unprotonated) amine groups was relatively small, resulting in a mixed monolayer of biotin-terminated thiol and amine-terminated thiol. The average area per biotin-terminated thiol in the mixed monolayer should be approximately equal to the projected area of avidin.¹⁰ Finally, the terminal biotin groups were reacted with fluorescently labeled avidin. The biotin–avidin linkage is one of the strongest known biological interactions with a binding constant of 10^{-15} M^{-1} and stability over a broad pH range.¹¹ Further details of experimental procedures can be found in the Supporting Information.

The initial fluorescence image in Figure 2a shows that the electrodes are uniformly functionalized with avidin. Two electrodes from the protein array were biased at -1.5 V (Ag/AgCl) for 90 s in phosphate-buffered saline (PBS, pH 7.4) resulting in desorption of the SAM and diffusion into bulk solution, as evidenced by the complete loss of fluorescence. Using this platform, biotinylated polymers, proteins, and

peptides can be tethered and hence their patterning and release can be readily controlled.

Figure 2b shows the electrochemically programmed release of 40 nm polystyrene nanoparticles conjugated with avidin under the same conditions. In these experiments, the avidin-conjugated nanoparticles were bound to the surface via a biotin linkage as described above. The loss of fluorescence illustrates successful release of the conjugated nanoparticles from one of the electrodes in the array. We have also achieved the controlled release of 200 nm amine-modified polystyrene particles conjugated directly to succinimide-terminated thiols at -1.3 V (Ag/AgCl) for 60 s in PBS. These examples mimic carriers for gene delivery that are often polycationic complexes or nanoparticles with surface amine moieties, and also vehicles for encapsulated small molecules (here fluorescent dyes and proteins, but which can also be drugs and catalytic compounds).

Since proteins and hydrophobic molecules tend to bind nonspecifically to gold surfaces,¹² control experiments were performed on unmodified gold electrodes. The extent of avidin immobilization due to nonspecific binding on bare gold was negligible compared to functionalized surfaces, and from the fluorescence images there was no evidence of electrochemical desorption, thereby highlighting the specificity of electrode loading and release. Nonspecific binding of nanoparticles was more extensive; however, no desorption was observed under conditions for electrochemical release. Thus, for the desorption experiments involving nanoparticles, nonspecific binding was minimized by suspending the particles in PBS with 1% bovine serum albumin which blocked the hydrophobic domains and hence enabled complete desorption from the electrodes.

The kinetics of protein release were determined from real-time fluorescence imaging. (A representative movie of the desorption process is provided in Supplementary Information). The results are summarized in Figure 3. Figure 3a shows a representative plot of the fluorescence intensity from a gold electrode versus the electrode potential for a mixed monolayer of avidin-terminated thiol and amine-terminated thiol. In this plot the potential was decreased by 50 mV every 25 s with the intensity recorded concurrently and this, as we show below, represents the dynamic response. The onset of desorption occurs at -0.85 V and the intensity decreases until -1.15 V . The intensity then remains constant until -1.45 V after which it steadily decreases to zero with increasing negative potential. We note that at this pH, the onset of visible hydrogen gas evolution on the bare gold surface occurred at about -1.6 V .

Figure 3b shows a cyclic voltammogram for a mixed monolayer of biotin-terminated thiol and amine-terminated thiol in PBS. From the voltammogram, the onset of reductive desorption is seen at about -0.85 V , corresponding to the onset of the decrease in the fluorescence intensity (Figure 3a). The reductive desorption process is complete at -1.15 V , coinciding with the onset of the plateau region in Figure 3a. At this potential, the monolayer is desorbed from the surface but is not immediately transported away from the surface. Thus the residual intensity in the plateau region is

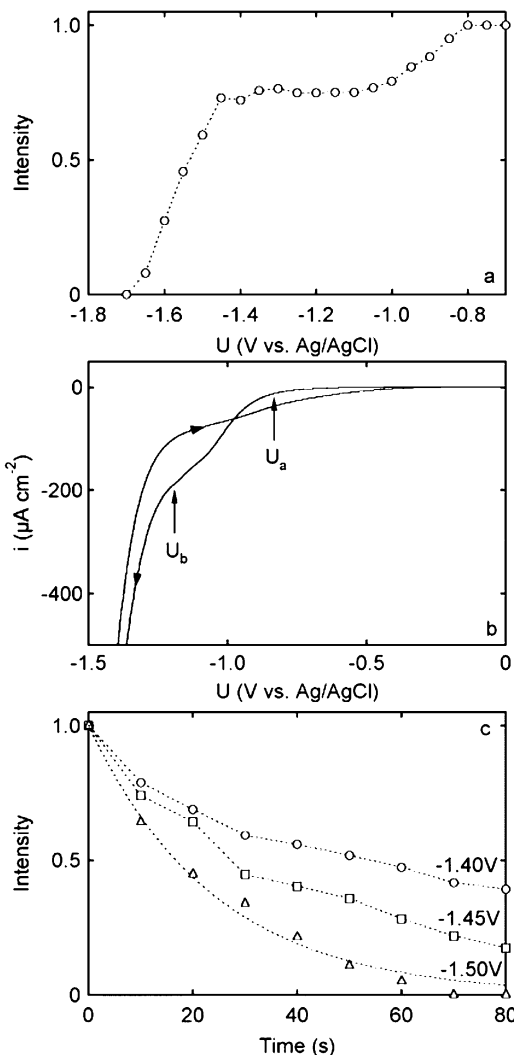


Figure 3. (a) Fluorescence intensity versus potential for an avidin-modified gold electrode in PBS. The fluorescence was obtained at 50 mV increments after 25 s. (b) Cyclic voltammogram for a modified gold electrode in PBS at a scan rate of 20 mV s^{-1} . The onset and completion of desorption are indicated by U_a and U_b , respectively. (c) Fluorescence intensity versus time for avidin-modified gold electrodes at -1.40 , -1.45 , and -1.50 V . All experiments were performed on polycrystalline gold with a mixed monolayer of biotin-terminated thiol and amine-terminated thiol, as described in the text.

due to desorbed avidin-terminated thiolates that are immobilized in domains of the biotin-terminated thiolate through lateral hydrophobic interactions. This is consistent with the hypothesized two-step desorption mechanism involving an initial one-electron reduction of the thiol to the thiolate at the electrode surface (eq 1), followed by the subsequent transport of the thiolate away from the surface at a rate that depends on the bulk solubility of the thiol.¹³

Figure 3c shows representative intensity versus time curves for an avidin-modified gold electrode at -1.4 , -1.45 , and -1.5 V . At -1.4 V the fluorescence shows complex desorption behavior due to the slow transport away from the surface, as described above. At -1.5 V , the fluorescence intensity decays exponentially to zero corresponding to complete desorption and transport away from the electrode after 70 s. Comparison to the voltammogram (Figure 3b)

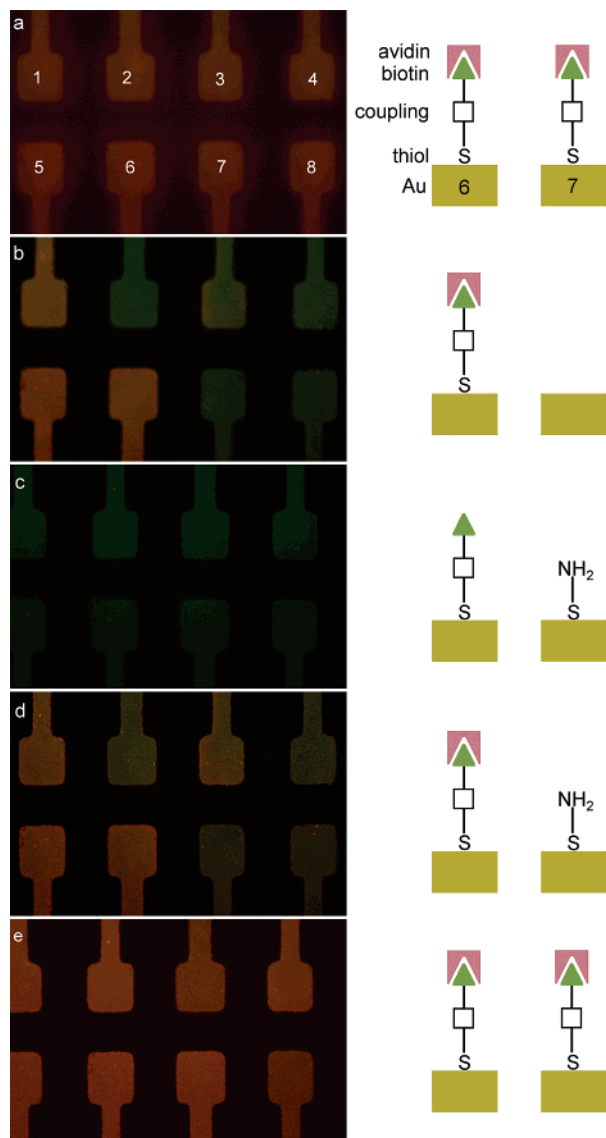


Figure 4. Electrode regeneration. Fluorescence images of (a) an avidin-modified gold electrode, (b) electrochemically programmed release from electrodes 2, 4, 7, and 8, and partial release from electrode 3, (c) removal of avidin from remaining electrodes (1, 5, and 6) in DMSO followed by the formation of an amine-terminated thiol monolayer on the bare gold electrodes (2, 4, 7, and 8), (d) the introduction of avidin results in strong emission from the electrodes with biotin-terminated thiol (1, 5, and 6) and weak fluorescence from electrodes with amine-terminated thiol due to nonspecific (electrostatic) interactions, and (e) reaction of a fraction of the amine-terminated thiols on electrodes 2, 4, 7, and 8 with succinimide-terminated biotin followed by reaction with avidin, resulting in complete regeneration of the electrodes.

suggests that the relatively fast exponential decay at -1.5 V and more negative potentials is assisted by concomitant hydrogen evolution. From the fit to the curve at -1.5 V , we obtain a rate constant of 0.042 s^{-1} and a half-time of 17 s.

The electrochemical desorption process results in recovery of the bare gold electrode surface, thus facilitating regeneration of the device as well as allowing sequential loading of different molecules and nanoparticles on different electrodes. Figure 4 demonstrates this concept. The gold electrodes were first modified with avidin resulting in uniform fluorescence

from all the electrodes (Figure 4a). Desorption from selected electrodes (2, 4, 7, and 8) resulted in the loss of fluorescence, as shown in Figure 4b. One electrode (3) was partially desorbed resulting in some residual fluorescence. Subsequently, the electrodes were rinsed with dimethyl sulfoxide (DMSO) to remove the avidin from the biotin-terminated thiol on electrodes that had not been desorbed. Introduction of amine-terminated thiol in DMSO results in the formation of a SAM of the amine-terminated thiol on the bare gold electrodes (see Figure 4c). Next, exposure to avidin results in fluorescence from the electrodes with biotin-terminated thiol SAMs (1, 5, and 6) that had not been desorbed. At the same time, nonspecific binding of the avidin to the protonated amines on the electrodes that had been desorbed results in weak fluorescence (see Figure 4d). Finally, addition of the succinimide-terminated biotin linker results in the formation of biotin terminations on the amine-terminated thiol and introduction of avidin results in complete regeneration of the protein array (Figure 4e). The ability to regenerate the electrodes makes this technique a versatile tool for both programmed capture and release of multiple molecules and/or carriers from individually addressable electrode arrays.

Additional features of this technique are the spatial control of the programmed release of one or more agents and the release of very small quantities. The concentration of thiols on gold is about 7.7×10^{-10} mol cm⁻² (4.6×10^{14} cm⁻²),¹⁴ and thus release of femtomolar concentrations can be readily attained with standard microfabrication techniques. Even smaller concentrations can be achieved by functionalizing the electrode with a mixed monolayer including a thiol that is not conjugated with the molecule or particle of interest.

We have also performed experiments in a two-electrode configuration that would be convenient for standalone microfluidic and drug release devices. For the protein array devices (Figure 2a) with a platinum counter electrode, the onset of the decrease in fluorescence occurred at -2.5 V, and a voltage of -2.7 V for about 30 s was sufficient to completely remove the chemisorbed SAMs.

In summary, we have demonstrated electrochemically programmed release of protein arrays and nanoparticle arrays. These devices are small, low power, low cost, easily loaded,

and can be regenerated. They have relatively fast response times, have no moving parts, and are biocompatible.¹⁵ We anticipate potential applications in drug delivery, lab-on-a-chip devices, and fundamental research requiring spatially controlled release¹⁶ and the ability to achieve ultralow concentrations.

Acknowledgment. P.M. thanks Bridget Wildt for several helpful discussions. This work was supported by the JHU MRSEC (NSF Grant No. DMR05-20491), and a graduate fellowship from the Whitaker Foundation. Correspondence and requests for materials should be addressed to P.C.S.

Supporting Information Available: Detailed description of the materials and methods and a video of the desorption process. This material is available free of charge via the Internet at <http://pubs.acs.org>.

References

- (1) Santini, J. T.; Cima, M. J.; Langer, R. *Nature* **1999**, *397*, 335–338.
- (2) Isalan, M.; Santori, M. I.; Gonzalez, C.; Serrano, L. *Nat. Methods* **2005**, *2*, 113–118.
- (3) Heller, M. J.; Tu, E. US Patent 5,605,662, 1997.
- (4) Rigaut, G.; Shevchenko, A.; Rutz, B.; Wilm, M.; Mann, M.; Seraphin, B. *Nat. Biotechnol.* **1999**, *17*, 1030–1032.
- (5) Lee, C. C.; Sui, G. D.; Elizarov, A.; Shu, C. Y. J.; Shin, Y. S.; Dooley, A. N.; Huang, J.; Daridon, A.; Wyatt, P.; Stout, D.; Kolb, H. C.; Witte, O. N.; Satyamurthy, N.; Heath, J. R.; Phelps, M. E.; Quake, S. R.; Tseng, H. R. *Science* **2005**, *310*, 1793–1796.
- (6) Ulman, A. *Chem. Rev.* **1996**, *96*, 1533–1554.
- (7) Widrig, C. A.; Chung, C.; Porter, M. D. *J. Electroanal. Chem.* **1991**, *310*, 335–359.
- (8) Yang, D. F.; Wilde, C. P.; Morin, M. *Langmuir* **1997**, *13*, 243–249.
- (9) Wong, S. S.; Porter, M. D. *J. Electroanal. Chem.* **2000**, *485*, 135–143.
- (10) Spinke, J.; Liley, M.; Guder, H. J.; Angermaier, L.; Knoll, W. *Langmuir* **1993**, *9*, 1821–1825.
- (11) Diamandis, E. P.; Christopoulos, T. K. *Clin. Chem.* **1991**, *37*, 625–636.
- (12) Mrksich, M.; Whitesides, G. M. *Annu. Rev. Biophys. Biomol. Struct.* **1996**, *25*, 55–78.
- (13) Pesika, N. S.; Stebe, K. J.; Searson, P. C. *Langmuir* **2006**, *22*, 3474–3476.
- (14) Schlenoff, J. B.; Li, M.; Ly, H. J. *Am. Chem. Soc.* **1995**, *117*, 12528–12536.
- (15) Merchant, B. *Biologicals* **1998**, *26*, 49–59.
- (16) Jiang, X.; Bruzewicz, D. A.; Wong, A. P.; Piel, M.; Whitesides, G. M. *Proc. Natl. Acad. Sci.* **2005**, *102*, 975–978.

NL0609302